Research Article

Jingjing Sun, Haibo Jin*, Xuefeng Mao, Guangxiang He, Junfang Li, Zihao Yan, Fating Hu, Lei Ma, Xiaoyan Guo, and Suohe Yang

The catalytic characteristics of 2-methylnaphthalene acylation with $AlCl_3$ immobilized on Hβ as Lewis acid catalyst

https://doi.org/10.1515/gps-2023-0003
received September 04, 2022; accepted December 02, 2022

Abstract: The heterogeneous supported Lewis acid catalyst prepared by immobilization technology has high reaction activity. It is an environment-friendly catalyst. Using Lewis acid immobilized as the catalyst, 2-methyl-6-propionyl naphthalene is synthesized by Friedel–Crafts reaction with 2-methylnaphthalene and propionic anhydride, which has a good development prospect. A variety of $AlCl_3$ catalysts supported by H-zeolite molecular sieves are prepared using the solvent reflux method in the paper. It is found that $AlCl_3$/Hβ has better catalytic performance. The results showed that $AlCl_3$/Hβ catalyst is mainly composed of L acid. The acid content of B acid and the specific surface area increase, and the pore volume and pore size decreases. With the increase in $AlCl_3$ concentration, the acid content of strong acid, medium strong acid, and weak acid increases, but the solubility of $AlCl_3$ in $CHCl_3$ is limited. When the concentration of $AlCl_3$ is too high, too much $AlCl_3$ is deposited on the surface of the molecular sieve, which is useless to its binding with Si–OH. $AlCl_3$/Hβ's activity is higher when the concentration of $AlCl_3$ is 3 g·L^{-1}, and the solvent is refluxed for 8 h and calcined at 550°C for 3 h. Under these conditions, the conversion of 2-methylnaphthalene is 85.86%, and the yield of β,β-methyl propyl naphthalene is increased to 81.19%.

Keywords: 2-methylnaphthalene, β,β-methyl propyl naphthalene, acylation, immobilized $AlCl_3$, zeolite molecular sieve

1 Introduction

β,β-Methyl propyl naphthalene is an important organic chemical raw material. The 2-methyl-6-propionyl naphthalene (2,6-MPN) is oxidized with ethylene glycol to obtain polyethylene 2,6-naphthalene dicarboxylate (PEN). It is a high-end polyester with excellent physical and chemical properties [1–6]. The synthesis method of 2,6-MPN mainly uses Lewis acid anhydrous $AlCl_3$ as the catalyst to catalyze the Friedel–Crafts acylation reaction between 2-methylnaphthalene (2-MN) and propyl chloride [7–9]. Li et al. [10] used an anhydrous $AlCl_3$ catalyst to carry out the 2-MN acylation reaction in a stainless-steel microchannel reactor, which had a high heat transfer rate. The yield of 2,6-MPN is 85.8%, and the selectivity is 87.5%. Although anhydrous $AlCl_3$ has good catalytic activity, it also has many shortcomings, such as large consumption, severe pollution, equipment corrosion, non-regeneration, and poor safety [11–13]. Therefore, it is urgent to develop a new acylation catalyst and green synthesis process of 2,6-MPN. The immobilized $AlCl_3$ catalyst can maintain the high catalytic activity of $AlCl_3$ and overcome the shortcomings of $AlCl_3$ decomposition in water, which is an ideal heterogeneous catalyst [14–22]. There are two methods to prepare an immobilized $AlCl_3$ catalyst: the physical adsorption method and the chemical bonding method [23–26]. Chemical bonding refers to the bonding between $AlCl_3$ and the hydroxyl group on the surface and the removal of the HCl molecule to obtain a heterogeneous catalyst containing $AlCl_3$.

* **Corresponding author: Haibo Jin,** Department of Chemical Engineering, School of New Materials and Chemical Engineering, Beijing Institute of Petrochemical and Technology/Beijing Key Laboratory of Fuels Cleaning and Advanced Catalytic Emission Reduction Technology, Beijing 102617, China, e-mail: jinhaibo@bipt.edu.cn
Jingjing Sun, Guangxiang He, Zihao Yan, Lei Ma, Xiaoyan Guo, Suohe Yang: Department of Chemical Engineering, School of New Materials and Chemical Engineering, Beijing Institute of Petrochemical and Technology/Beijing Key Laboratory of Fuels Cleaning and Advanced Catalytic Emission Reduction Technology, Beijing 102617, China
Xuefeng Mao, Junfang Li, Fating Hu: Laboratory of Coal based High Energy Fuel and Fine Chemicals, Beijing Research Institute of Coal Chemistry, CCTEG Coal Research Institute, Beijing 100013, China

There are two main methods to immobilize $AlCl_3$ by chemical bond: the gas phase method [27] and the liquid phase method [22,28–30]. $AlCl_3$ is easy to sublimate, and N_2 is used to react with zeolite molecular sieve and other carriers to form the immobilized $AlCl_3$. The experimental operation is simple, but the equipment is too high to realize. The liquid phase method dissolves $AlCl_3$ in halogenated alkane solvent and reacts with the carrier for a period to generate the embedded $AlCl_3$. The solvent used in the liquid phase reaction is toxic, but the operation is simple. Both methods of immobilized $AlCl_3$ have been presented, and the prepared immobilized $AlCl_3$ catalyst has good catalytic activity in many organic reactions, especially Friedel–Crafts reactions. In this article, a series of catalysts were prepared using H-zeolite molecular sieves as carriers and using the solvent reflux method to immobilize $AlCl_3$ under different conditions. The preparation conditions and the catalytic performance of the 2-MN acylation reaction were studied. This is a new green catalytic process, which can accelerate the research and production process of PEN and improve people's quality of life.

2 Experimental

2.1 Preparation of $AlCl_3$ supported catalyst

The zeolite molecular sieve was pretreated in a muffle furnace at 600°C for 3 h. Anhydrous $AlCl_3$ was weighed and placed in a 250 mL three-way flask. Then, 100 mL $CHCl_3$ solution was added. After nitrogen was pumped in and the air was emptied, the metal bath controller was turned on to stir. After $AlCl_3$ was fully dissolved, 10 g of pretreated zeolite molecular sieve (sieve agent ratio 1:10) was added and stirred at a high temperature to reflux the solvent. After a while, the heating was stopped. The three-end flask was cooled to room temperature, filtered, and washed with $CHCl_3$. The solid was placed in a vacuum oven at 50°C overnight. After grinding, it was roasted at 550°C for 3 h in a muffle furnace and cooled to room temperature. Finally, the immobilized $AlCl_3$ catalyst was obtained.

2.2 Characterization of the supported catalyst

Acidity was determined using an automatic temperature-programmed chemisorption (NH_3-TPD) unit developed by Micromeritics (AutoChem II 2920) with a thermal conductivity detector (TCD). The 0.2 g catalyst sample was first flushed with helium (30 mL·min^{-1}) at 700°C for 3 h, cooled to 150°C, saturated with NH_3 until equilibrated, and then flushed again with helium until the baseline of the integrator was stable. The NH_3-TPD treatment quickly starts from 150°C to 700°C, and the heating rate was 15°C·min^{-1}. Surface morphology was observed using the TESCAN MIRA4 ultra-high resolution field emission scanning electron microscope (SEM) manufactured in the Czech Republic. The electron gun was a Schottky field emission gun, the magnification was 2–50 k, and the test voltage was 30 kV.

Specific surface area and pore volume aperture (BET) were measured using Micromeritics ASAP 2460 3.01. About 0.12 g of the sample was weighed into a sample tube, vacuum-dried, and then de-vacuumed (300°C degassing for 3 h), and then N_2 was adsorbed in liquid nitrogen −196°C. After the test was completed, the specific surface area of the catalyst was calculated by the BET method. The BJH model calculated the pore size distribution.

A PANalytical Axios X-ray fluorescence spectrometer (XRF) produced by Philips was used to determine the contents of each component in the catalyst. The instrument type was multi-channel, and the power of the X-ray was 4 kW. Pyridine absorption infrared spectroscopy (Py-IR) used a Thermo Fisher Nicolet iS50 infrared spectrometer to measure the concentration of Brönsted and Lewis acids in the samples. The transmission method was used for testing, the number of infrared scanning was 32 times, the scanning wavelength was 400–4,000 cm^{-1}, and the resolution was 4 cm^{-1}.

2.3 Catalyst evaluation

A certain amount of 2-MN and propionic anhydride (PA) were added to a three-necked round-bottomed flask equipped with a condenser tube, a thermometer, a drying tube, and a metal bath. Then, an appropriate amount of solvent was added. After stirring evenly, the catalyst was added, and the temperature was raised and stirred continuously for a while. Then, the catalyst was separated by filtration, and the reaction solution was analyzed using a gas chromatograph.

GC-2014C (SHIMADZU, Japan) was equipped with an FID detector. The temperature program mode (215°C for 30 min) was used to analyze the extracted reaction solution. The chromatographic column was HP-5 50 m × 0.20 mm. N_2 was used as carrier gas at the nitrogen pressure of 0.5 MPa. The detector temperature was 300°C, and the injection port temperature was 300°C. The injection quantity was 0.2 μL.

3 Results and discussion

3.1 Effect of different molecular sieve carriers on 2-MN acylation catalyzed by $AlCl_3$

Five H-zeolite molecular sieves USY (SiO_2/Al_2O_3 = 6), HY (SiO_2/Al_2O_3 = 6), meridians (MOR: SiO_2/Al_2O_3 = 10), HZSM-5 (SiO_2/Al_2O_3 = 25), and Hβ (SiO_2/Al_2O_3 = 25) were used as carriers to prepare the immobilized $AlCl_3$ catalyst under the same conditions, which was used to catalyze the acylation reaction of 2-MN with PA. Tetramethylene sulfone (TS) was used as the solvent. The results are shown in Table 1.

Hβ zeolite molecular sieve as a carrier of $AlCl_3$ had significantly more vigorous catalytic activity than other zeolite molecular sieves, with a higher conversion of 2-MN and a selectivity of β,β-MPN up to 94.4%. There were two possible reasons: on the one hand, Hβ had open three-dimensional channels, the pore size was much larger than HZSM-5, PA could freely access Hβ channels, $AlCl_3$/Hβ surface-active center was completely contacted, and chemical adsorption could form a large number of acyl carbocation, conducive to the reaction; on the other hand, Hβ itself had a large number of medium and strong acids that promoted Friedel–Crafts acylation reaction between 2-MN and PA, and its acidity was much more than HY, USY, MOR, and HZSM-5, which was the main reason why $AlCl_3$/Hβ had more vital catalytic activity than other zeolite molecular sieves immobilized $AlCl_3$. However, other zeolite molecular sieves had less strong acid and limited $AlCl_3$ load, so the active intermediates generated on the active center were inadequate to attack the inert aromatic ring, resulting in low catalytic activity. Therefore, the Hβ zeolite molecular sieve (Si/Al ratio of 25) was used as the carrier to prepare $AlCl_3$/Hβ catalyst.

Table 1: Effect of different zeolite carriers on 2-MN propionyl catalyzed by $AlCl_3$

Catalysts	Conversion (%)	Selective (%)		
		2,6-MPN	2,7-MPN	Others
$AlCl_3$/USY	49.6	41.8	25.7	32.5
$AlCl_3$/HY	55.0	34.3	12.5	53.2
$AlCl_3$/MOR	48.1	21.7	9.8	68.5
$AlCl_3$/HZSM-5	49.7	23.4	23.5	53.1
$AlCl_3$/Hβ	76.2	48.0	46.4	5.6

Reaction conditions: 2-MN 0.0125 mol, PA 0.025 mol, TS 10 g, catalyst (calcination at 600°C for 3 h) 3 g, 190°C, 10 h.

3.2 Characterization analysis of $AlCl_3$/Hβ catalyst

3.2.1 XRD characterization of $AlCl_3$/Hβ catalysts prepared with different concentrations of $AlCl_3$

The $AlCl_3$/Hβ catalysts prepared by the solvent reflux method with different concentrations of $AlCl_3$ were characterized by XRD. According to the results in Figure 1, the XRD diffraction peaks of $AlCl_3$/Hβ catalysts prepared with different concentrations of $AlCl_3$ showed the standard diffraction peaks of Hβ (PDF # 48-0074). Moreover, the peak pattern was sharp, indicating that the crystal phase of Hβ was undamaged in the modification process, and the crystal phase was intact. There was no diffraction peak of $AlCl_3$ in the figure, and the skeleton structure of the catalyst was still Hβ, indicating that $AlCl_3$ existed in an amorphous form in the $AlCl_3$/Hβ catalyst and $AlCl_3$ was well dispersed in Hβ. Compared with Hβ, the diffraction peak intensity of the catalyst with $AlCl_3$ immobilized was more vigorous overall. The diffraction peak intensity of the catalyst immobilized with 1 g·L^{-1} $AlCl_3$ had a non-significant difference from the unmodified Hβ. The diffraction peak of $AlCl_3$/Hβ catalyst with an $AlCl_3$ concentration of 1 g·L^{-1} was inconspicuous from that of unmodified Hβ.

3.2.2 SEM characterization of $AlCl_3$/Hβ catalysts prepared with different concentrations of $AlCl_3$

SEM characterized the $AlCl_3$/Hβ catalysts obtained with different concentrations of $AlCl_3$, and the results are shown in Figure 2.

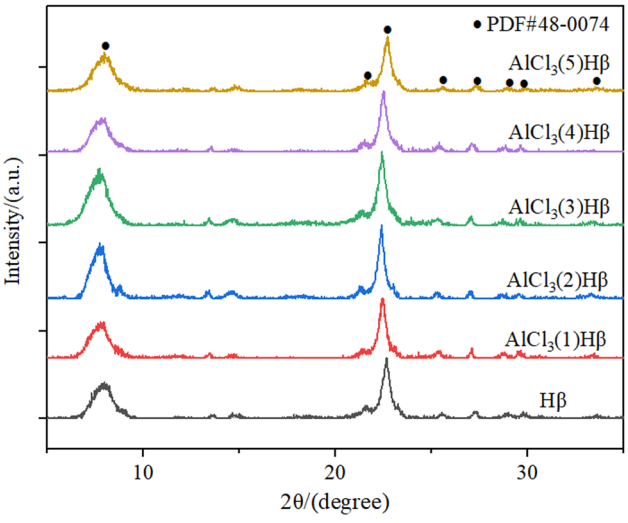

Figure 1: XRD patterns of $AlCl_3$/Hβ catalysts prepared with different concentrations of $AlCl_3$.

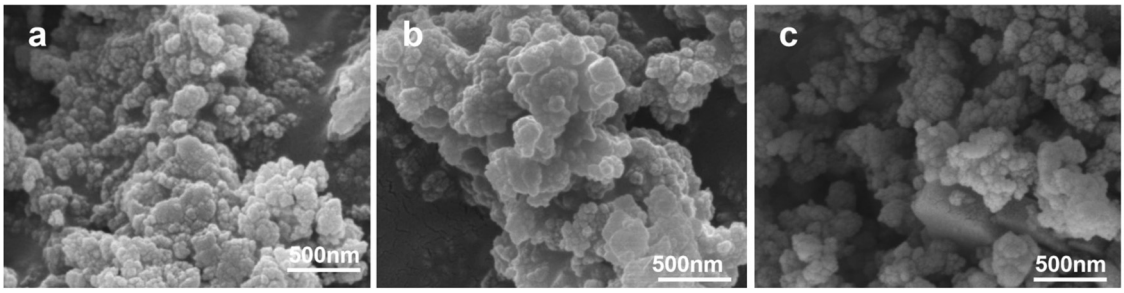

Figure 2: SEM of $AlCl_3$/Hβ catalysts prepared with different concentrations of $AlCl_3$: (a) $AlCl_3$ (1 g·L^{-1})/Hβ, (b) $AlCl_3$ (3 g·L^{-1})/Hβ, and (c) $AlCl_3$ (5 g·L^{-1})/Hβ.

The $AlCl_3$/Hβ catalyst particles were small cubes, but the size distribution of surface particles was uneven, and there was an agglomeration phenomenon. With the increase in $AlCl_3$ concentration, the tiny particles immobilized on the surface of the 3 g·L^{-1} $AlCl_3$-modified Hβ became more extensive. The distribution was relatively uniform compared with that of 1 g·L^{-1} void became smaller. As the concentration of $AlCl_3$ increased, the surface particles increased, the voids continued to decrease, and some pores were blocked, which was adverse to catalyzing the 2-MN acylation reaction.

3.2.3 BET characterization of $AlCl_3$/Hβ catalysts prepared with different concentrations of $AlCl_3$

The effect of different concentrations of $AlCl_3$ loading on the specific surface area, pore volume, and pore size distribution of Hβ was studied, and the BET characterization was carried out. The results are shown in Table 2.

Compared with the unmodified Hβ, the Hβ-specific surface area of $AlCl_3$ supported by solvent reflux increased significantly with $AlCl_3$ concentration. The reason can be explained that the load increases with the concentration increasing of $AlCl_3$. Combined with SEM results, it was shown that the number of small particles on the surface increased, resulting in an increase in specific surface area and a decrease in pore volume and pore size. It may be due to the reaction between $AlCl_3$ and Si–OH on the surface of zeolite, resulting in the reduction of pore size. When the concentration of $AlCl_3$ continued to increase, the particles on the surface gradually increased. The bonding between the bonds leads to a decrease in the specific surface area, pore volume, and aperture. In addition, due to the high concentration of $AlCl_3$ load, $AlCl_3$/Hβ catalyst appeared to sinter after calcination, which was also one reason for reducing the specific surface area. At the same time, the results characterized by BET also showed that the specific surface area was the largest, and the void space of the catalyst was rich and uniform when the $AlCl_3$ concentration was 3 g·L^{-1}.

3.2.4 NH_3-TPD characterization of $AlCl_3$/Hβ catalysts prepared with different concentrations of $AlCl_3$

NH_3-TPD spectra of $AlCl_3$/Hβ catalysts prepared with different concentrations of $AlCl_3$ are shown in Figure 3.

Compared with the unmodified Hβ zeolite molecular sieve, with the increase in $AlCl_3$ concentration, the strong acid strength and acid content of $AlCl_3$/Hβ only changed slightly. In general, there was still an increase in acid content. It may be due to the increase in the number of L-acid sites, which happened to be caused by strong acid sites, thus increasing acid strength and acid content. However, as the concentration of $AlCl_3$ continued to increase, the strength of strong acid was unchanged,

Table 2: BET characterization results of $AlCl_3$/Hβ catalysts prepared with different concentrations of $AlCl_3$

Catalysts	Surface area ($m^2 \cdot g^{-1}$)	Micropore area ($m^2 \cdot g^{-1}$)	External surface area ($m^2 \cdot g^{-1}$)	Pore volume ($cm^3 \cdot g^{-1}$)	Micropore volume ($cm^3 \cdot g^{-1}$)	Mesoporous volume ($cm^3 \cdot g^{-1}$)	Pore size (nm)
Hβ	530	358	172	0.45	0.17	0.29	4.63
$AlCl_3$(1)/Hβ	534	362	172	0.44	0.17	0.27	4.63
$AlCl_3$(3)/Hβ	559	376	183	0.45	0.16	0.25	4.50
$AlCl_3$(5)/Hβ	543	371	172	0.33	0.15	0.18	4.26

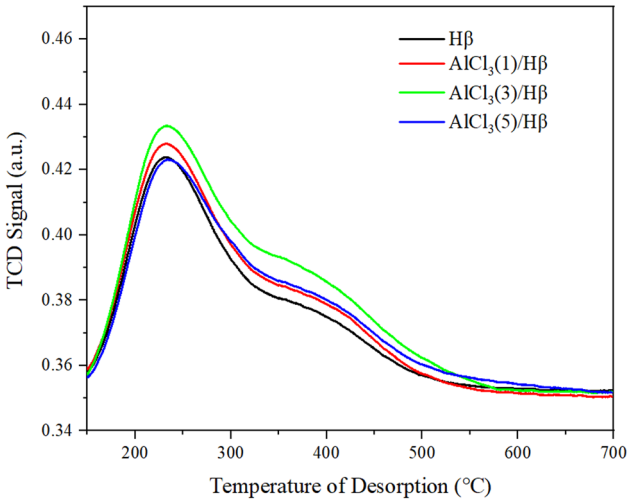

Figure 3: NH_3-TPD spectra of $AlCl_3$/Hβ catalysts prepared with different concentrations of $AlCl_3$.

but the acid content increased slightly. The strength of medium–strong acid increased compared with Hβ, but it was still slightly decreased compared with the Hβ molecular sieve loaded with 3 g·L^{-1} $AlCl_3$. The reason may be that the concentration of $AlCl_3$ was too high. The undissolved $AlCl_3$ was deposited on the surface of Hβ in a free state. Part of the $AlCl_3$ was sintered during calcining, destroying the part of the acid center.

3.2.5 Py-IR characterization of $AlCl_3$/Hβ catalysts prepared with different concentrations of $AlCl_3$

Pyridine adsorption infrared data of $AlCl_3$/Hβ catalysts prepared with different concentrations of $AlCl_3$ at different temperatures are shown in Figure 4.

To more intuitively compare the acidity of Hβ molecular sieves loaded with $AlCl_3$, the data of the pyridine infrared spectrum were summarized, as shown in Table 3.

Figure 4a–c corresponds to the changes in acid content and acid strength of $AlCl_3$/Hβ catalysts prepared at different concentrations of $AlCl_3$ at 150°C, 300°C, and 450°C, respectively. With the increase in $AlCl_3$ concentration, compared with strong acid and medium–strong acid, the increasing trend of weak acid was the largest, and the increasing trend of strong acid was also more extensive. The increasing trend of Lewis acid was more prominent than that of Bronsted acid. The main reason was that strong acid sites increased Lewis acid quantity, and $AlCl_3$ itself was a Lewis acid. With the further increase of $AlCl_3$ concentration, the medium and strong acid contents decreased, while the change in the Bronsted acid content was minor. As the concentration of $AlCl_3$ continued to increase, part of $AlCl_3$ attached to the surface of Hβ did not form chemical bonds with the surface elements. It is also reflected in the preparation process of

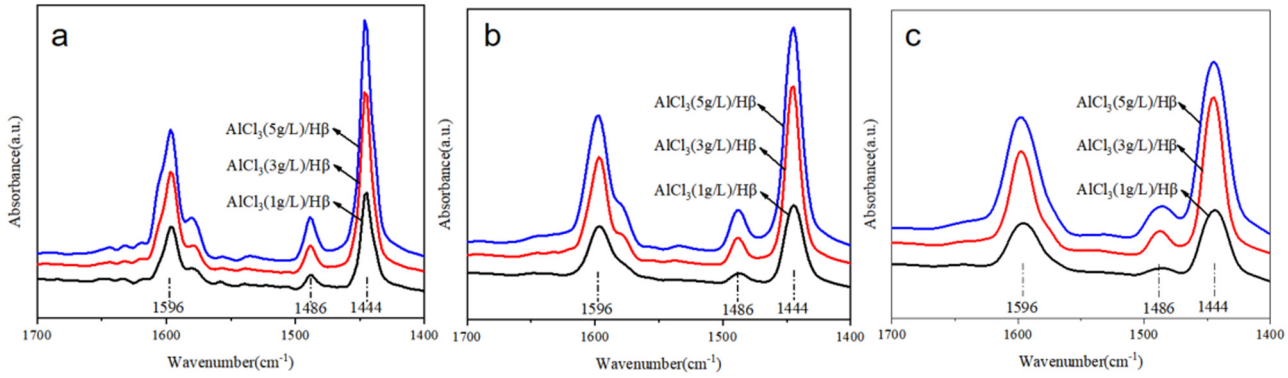

Figure 4: Py-IR spectra of $AlCl_3$/Hβ catalysts prepared with different concentrations of $AlCl_3$: (a) 150°C, (b) 300°C, and (c) 450°C.

Table 3: Py-IR data of $AlCl_3$/Hβ catalysts prepared with different concentrations of $AlCl_3$

Catalysts	Strong acid (μmol·g^{-1})			Mediate strong acid (μmol·g^{-1})			Weak acid (μmol·g^{-1})		
	Bronsted acid	Lewis acid	Total acid	Bronsted acid	Lewis acid	Total acid	Bronsted acid	Lewis acid	Total acid
$AlCl_3$(1)/Hβ	1.74	14.20	15.93	2.68	71.03	73.71	3.48	262.03	265.31
$AlCl_3$(3)/Hβ	2.06	65.69	67.75	6.45	176.15	182.60	9.49	401.30	410.79
$AlCl_3$(5)/Hβ	2.76	147.30	150.06	6.48	174.21	180.69	18.00	413.42	431.42

Table 4: Comparison of percentage content and ratio of $AlCl_3$/Hβ catalysts supported by different concentrations of $AlCl_3$

Catalysts	Al_2O_3 (wt%)	SiO_2 (wt%)	Cl (wt%)	SiO_2/Al_2O_3	Si (wt%)	Al (wt%)	Si/Al
Hβ	6.665	92.802	0	23.628	43.379	3.528	11.814
$AlCl_3$(1)/Hβ	9.709	89.562	0.094	15.654	88.600	10.219	8.328
$AlCl_3$(3)/Hβ	10.652	88.129	0.113	14.040	86.898	11.108	7.514
$AlCl_3$(5)/Hβ	11.716	87.592	0.111	12.687	86.702	12.178	6.838

increasing bonds mainly for Hβ molecular sieve increased the Bronsted acid center. The ratio of Bronsted acid and Lewis acid determines the increase of medium strong acid.

3.2.6 XRF characterization of $AlCl_3$/Hβ catalysts prepared with different concentrations of $AlCl_3$

For the supported zeolite catalyst, the Si/Al ratio and other components of the supported zeolite have a significant influence on the activity of the catalyst. Table 4 compares the percentage content and ratio of each component in $AlCl_3$/Hβ catalysts supported by different concentrations of $AlCl_3$.

The Si/Al ratio of Hβ immobilized with $AlCl_3$ decreased, the SiO_2/Al_2O_3 ratio of the modified zeolite decreased from 23.628 to 12.687, and the content of Cl remained unchanged. The percentage content of Cl increased gradually with the increase in $AlCl_3$ concentration. It indicated that the immobilized $AlCl_3$ was combined with the Si–OH on the surface of the Hβ molecular sieve. Qi et al. [26] used the ^{27}Al MAS NMR method to study the possible binding forms of $AlCl_3$ and Si–OH after immobilization in the molecular sieve, as shown in Figure 5.

Different concentrations of $AlCl_3$ may predominate $AlCl_3$/Hβ in one or more forms shown in Figure 5a–d. However, either form increased Cl in terms of acidity and acid strength, thus modulating the acidity of the catalyst, catalytic activity, and selectivity to the target product β,β-MPN.

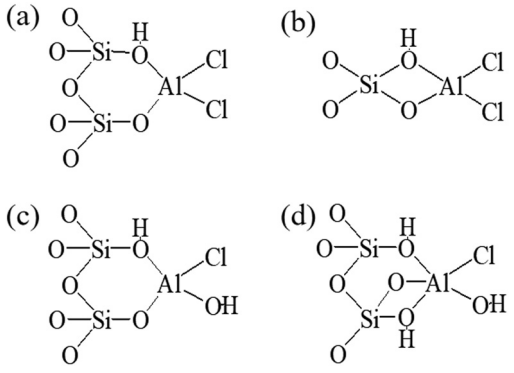

Figure 5: Possible binding form of $AlCl_3$ and Si–OH after loading on molecular sieve.

3.3 Effect of preparation conditions on propionyl of 2-MN catalyzed by $AlCl_3$/Hβ catalyst

3.3.1 Effect of $AlCl_3$ concentration on the catalytic performance of $AlCl_3$/Hβ

The effect of $AlCl_3$/Hβ catalysts prepared with different concentrations of $AlCl_3$ on the acylation reaction of 2-MN and PA is shown in Figure 6.

As shown in Figure 6, with the increase of $AlCl_3$ concentration, the conversion of 2-MN gradually increased and reached the highest point at 3 g·L^{-1}, which may be the maximum $AlCl_3$ loading capacity of the catalyst prepared at this concentration. However, when $AlCl_3$ was immobilized with Hβ, two B-acid sites were converted

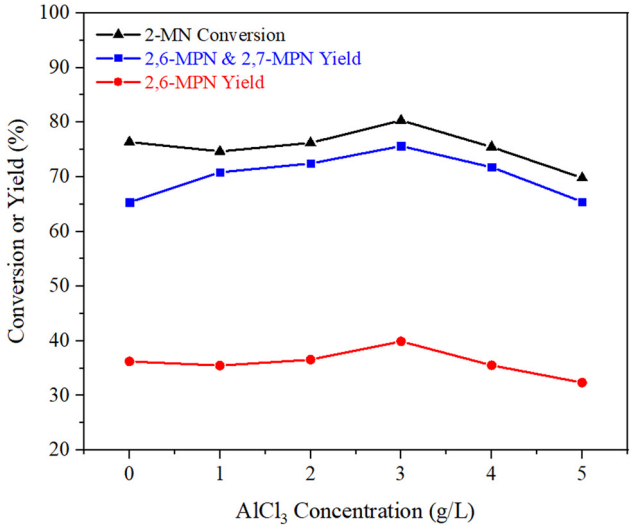

Figure 6: Effect of $AlCl_3$ concentration on the catalytic performance of $AlCl_3$/Hβ. Reaction conditions: $n_{(2\text{-MN})}$:$n_{(PA)}$ = 1:1.8, TS 10 g, $AlCl_3$/Hβ (reflux for 8 h and calcination at 550°C for 3 h) 3 g, 190°C, 10 h.

into one L-acid site. The total acid content showed an increasing trend, so the catalytic activity increased. In addition, the reaction between $AlCl_3$ and part of Si–OH in Hβ channels increased the pore size and the shape selectivity of $AlCl_3$/Hβ, which was conducive to the formation of 2,6-MPN. To further increase the concentration of $AlCl_3$, due to the high concentration part of $AlCl_3$ exhalation, deposition on the surface of Hβ, after calcining sintered parts, affects the catalytic activity of catalysts. It can be seen from the SEM in the figure that a high concentration of $AlCl_3$ Hβ surface structure of the load was affected, selectivity of the catalyst declined. Therefore, the appropriate concentration of $AlCl_3$ was 3 g·L^{-1}.

3.3.2 Effect of reflux time on the catalytic performance of $AlCl_3$/Hβ

The effect of $AlCl_3$/Hβ catalysts prepared at different load times on the 2-MN acylation reaction is shown in Figure 7. When Hβ zeolites were reflux reacted in $CHCl_3$ solution of $AlCl_3$ for 9 h, the conversion was the highest, 82.2%, but the selectivity of the target product 2,6-MPN was slightly reduced. When the load time was 8 h, the selectivity for 2,6-MPN was up to 49.7%, although the catalytic activity decreased. It may be because when the load time was 9 h, $AlCl_3$ had completely reacted with Si–OH on the pore surface, and part of $AlCl_3$ was attached to the surface. Although a large amount of $AlCl_3$ can catalyze the acylation of 2-MN, the decrease of pore size resulted in some β,β-MPN with larger molecular diameters trapped in the pore, and an increase of other by-products. Therefore, the appropriate load time was 9 h.

3.3.3 Effect of calcination temperature on the catalytic performance of $AlCl_3$/Hβ

The precursor of $AlCl_3$/Hβ catalyst prepared with $AlCl_3$ concentration of 3 g·L^{-1} at 60°C for 8 h was calcined in a muffle furnace. The effect of calcination temperature was investigated, and the results are shown in Figure 8. The conversion of 2-MN was almost unchanged with calcination temperature increasing, but the yield of 2,6-MPN increased gradually. When the calcination temperature was over 550°C, the yield of 2,6-MPN decreased, while the yield of β,β-MPN was almost unchanged. The reason may be that the calcination temperature was too high, and $AlCl_3$/Hβ could be partially sintered, destroying the surface acid center and affecting the catalytic activity. Therefore, the appropriate roasting temperature was 550°C.

3.3.4 Effect of calcination time on the catalytic performance of $AlCl_3$/Hβ

The results of calcination time are shown in Figure 9. It can be seen that calcination time had little effect on $AlCl_3$/Hβ. The conversion of 2-MN and the yield of β,β-MPN were the highest at 3 h. It showed that the structure of the carrier

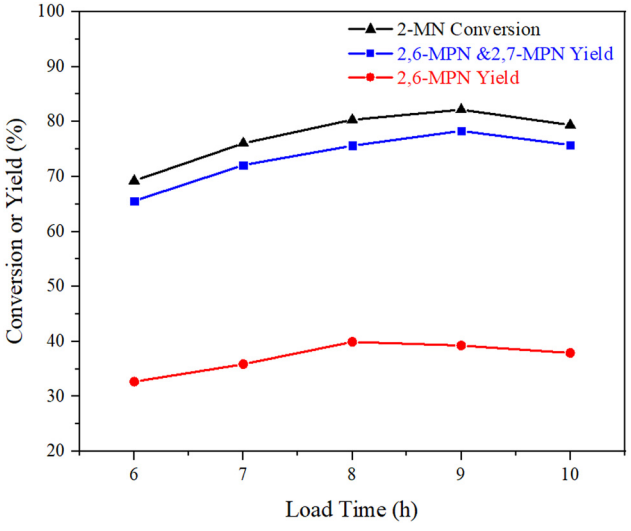

Figure 7: Influence of reflux time on catalytic performance of $AlCl_3$/Hβ. Reaction conditions: $n_{(2\text{-MN})}$:$n_{(PA)}$ = 1:1.8, TS 10 g, $AlCl_3$/Hβ ($AlCl_3$ 3 g·L^{-1} and calcination at 550°C for 3 h) 3 g, 190°C, 10 h.

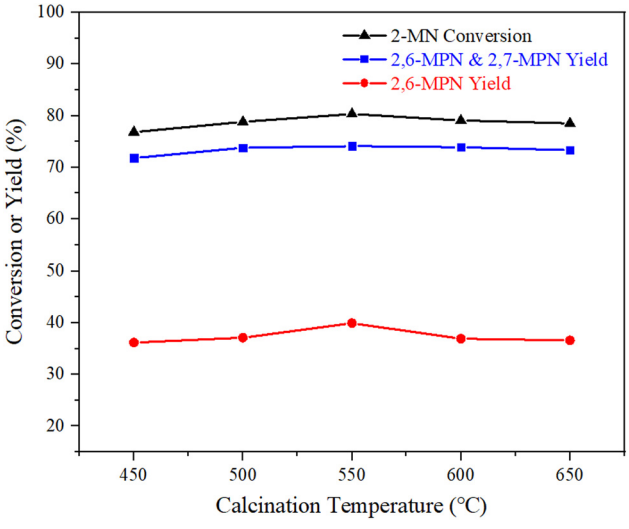

Figure 8: Influence of calcination temperature on the performance of 2-MN propionyl catalyzed by $AlCl_3$/Hβ. Reaction conditions: $n_{(2\text{-MN})}$:$n_{(PA)}$ = 1:1.8, TS 10 g, $AlCl_3$/Hβ ($AlCl_3$ g·L^{-1}, reflux for 9 h and calcination for 3 h) 3 g, 190°C, 10 h.

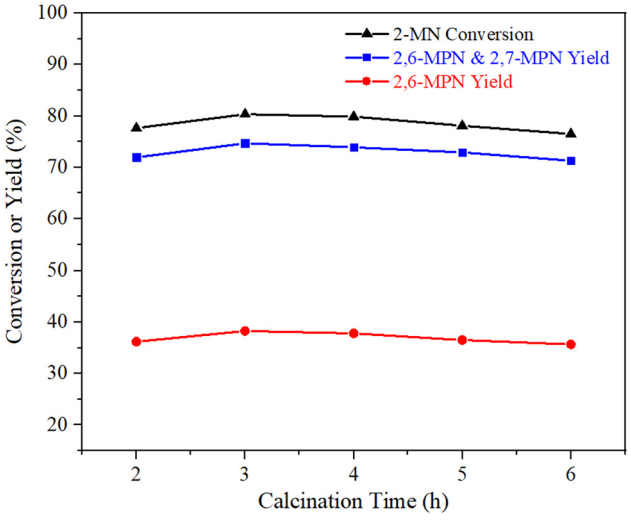

Figure 9: Effect of calcination time on the performance of 2-MN propionyl catalyzed by $AlCl_3$/Hβ. Reaction conditions: $n_{(2\text{-MN})}$:$n_{(PA)}$ = 1:1.8, TS 10 g, $AlCl_3$/Hβ ($AlCl_3$ 3 g·L^{-1}, reflux for 9 h and calcination at 550°C) 3 g, 190°C, 10 h.

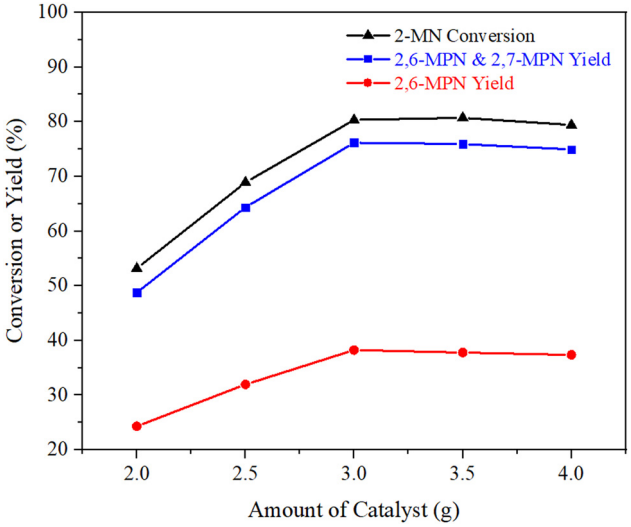

Figure 10: Influence of catalyst dosage on 2-MN propionylation reaction. Reaction conditions: $n_{(2\text{-MN})}$:$n_{(PA)}$ = 1:1.8, TS 10 g, $AlCl_3$/Hβ ($AlCl_3$ 3 g·L^{-1}, reflux for 9 h and calcination at 550°C for 3 h), 190°C, 10 h.

Hβ had been very stable. Therefore, the calcination time of 3 h was suitable.

3.4 Optimization of propionyl reaction conditions of 2-MN catalyzed by $AlCl_3$/Hβ catalyst

$AlCl_3$/Hβ catalyst was prepared with the $AlCl_3$ concentration of 3 g·L^{-1} at 60°C for 8 h and calcination at 550°C for 3 h to optimize the reaction conditions of 2-MN propyl acylation.

3.4.1 Effect of catalyst dosage on 2-MN propionyl reaction

The effect of catalyst dosage on 2-MN propionyl reaction was investigated, and the results are shown in Figure 10. When the dosage of $AlCl_3$/Hβ was 2 g, the conversion of 2-MN was only 53.2%, and the yield of β,β-MPN was also very low. With the increase of the dosage of $AlCl_3$/Hβ, the conversion of 2-MN showed a trend of continuous increase because the increase of $AlCl_3$/Hβ accelerated the acylation reaction of 2-MN with PA. The yield of 2-MPN was the highest when the dosage was 3 g. The 2-MN conversion increased, but the by-products increased obviously. Furthermore, too much catalyst would accelerate the occurrence of side reactions and significantly increase the cost of the reaction. Overall consideration, when the dosage of $AlCl_3$/Hβ was 3 g, it was suitable.

3.4.2 Effect of reaction temperature on propionyl of 2-MN

The acylation of 2-MN is an exothermic reaction. The temperature has a certain influence on the acylation reaction. Under the conditions of $n_{(2\text{-MN})}$:$n_{(PA)}$ = 1:1.8, TS 10 g, $AlCl_3$/Hβ 3 g, and reaction time 9 h, the effects of reaction temperature on the conversion of 2-MN and the selectivity of β,β-MPN were investigated. The experimental results are shown in Figure 11.

With the increase in reaction temperature, the transformation of 2-MN first increased and then decreased; the highest conversion was 82.9% at 190°C. It was because when the reaction temperature was increased in the range of 170–190°C, the movement rate of molecules in the reaction was accelerated, which made the reactants 2-MN, PA, and products 2,6-MPN, 2,7-MPN molecules more easily desorbed from $AlCl_3$/Hβ and reduced the accumulation of macromolecules. It could improve the catalytic performance of the $AlCl_3$/Hβ catalyst. Therefore, the reaction temperature of 190°C was appropriate.

3.4.3 Effect of reaction time on propionyl of 2-MN

Under the conditions of $n_{(2\text{-MN})}$:$n_{(PA)}$ = 1:1.8, TS 10 g, $AlCl_3$/Hβ 3 g, reaction temperature 190°C, the samples of different times were taken for GC detection to investigate the effect of reaction time on the conversion of 2-MN and the selectivity of β,β-MPN. The result is shown in Figure 12.

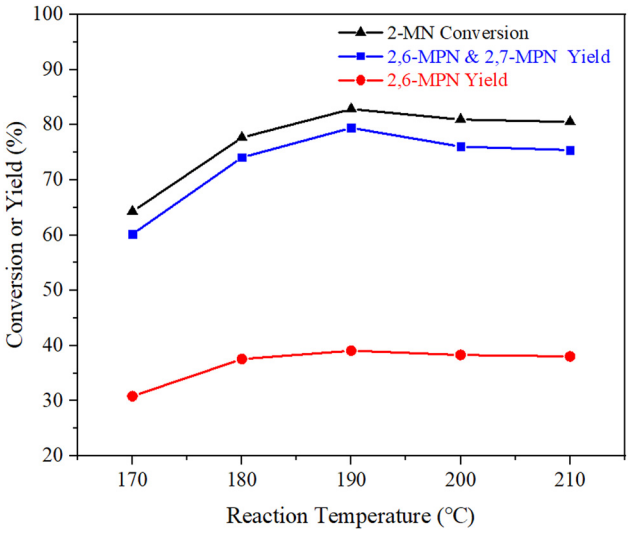

Figure 11: Effect of reaction temperature on propionylation of 2-MN. Reaction conditions: $n_{(2\text{-MN})}$:$n_{(PA)}$ = 1:1.8, TS 10 g, $AlCl_3$/Hβ ($AlCl_3$ 3 g·L^{-1}, reflux for 9 h and calcination at 550°C for 3 h) 3 g, 10 h.

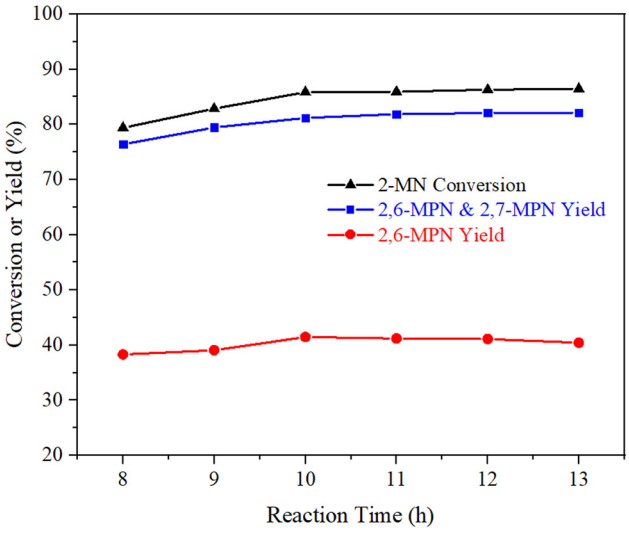

Figure 12: Effect of reaction time on propionylation of 2-MN. Reaction conditions: $n_{(2\text{-MN})}$:$n_{(PA)}$ = 1:1.8, TS 10 g, $AlCl_3$/Hβ ($AlCl_3$ 3 g·L^{-1}, reflux for 9 h and calcination at 550°C for 3 h) 3 g, 190°C, 10 h.

With the prolongation of reaction time, the conversion of 2-MN and the yield of β,β-MPN increased gradually. When the reaction time was 10 h, the maximum yield of 2,6-MPN was 41.5%. After that, when the reaction time was 11 h, the conversion of 2-MN and the yield of other β,β-MPN continued to increase, while the yield of 2,6-MPN decreased by 0.3%. As the reaction time continued to increase, the results were predictable: The conversion of 2-MN and other β,β-MPN yields continued to increase, while the yields of 2,6-MPN gradually decreased. It may be because the propionyl reaction of 2-MN in the reaction was intermittent, and 2,6-MPN, 2,7-MPN, 2,3-MPN, and other products coexisted in the product. As the reaction time increased, the generated products would be converted into other by-products, reducing 2,6-MPN [9]. Therefore, after careful consideration, the appropriate reaction time was 10 h.

3.5 Catalytic reaction feasible mechanism

The reaction mechanism of Friedel–Crafts acylation of 2-MN catalyzed by zeolite molecular sieve is still ambiguous. Yuan et al. [9] proposed that in the catalytic process

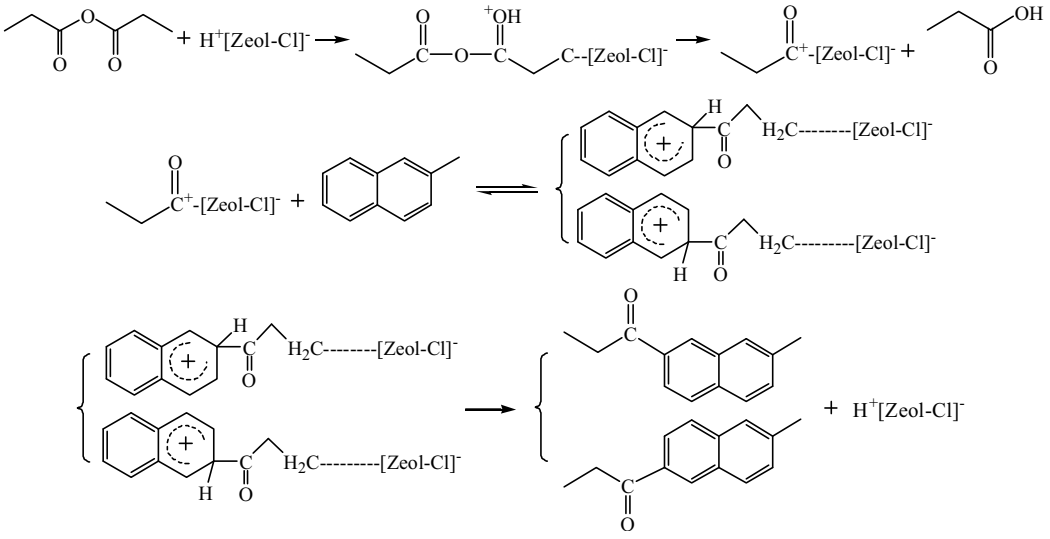

Figure 13: Mechanism of 2-MN propionyl catalyzed by zeolite molecular sieve.

of zeolite molecular sieve catalyst, medium strong acid played a significant role. The ratio of Bronsted acid to Lewis acid could effectively catalyze the acylation reaction of the aromatic ring within an appropriate range. And the acylation reaction process of 2-MN and anhydride catalyzed by zeolite molecular sieve was proposed, as shown in Figure 13.

The reaction mechanism of Hβ zeolite immobilized by $AlCl_3$ can be divided into two types according to the type of acid active center. One is a new acid active center formed by $AlCl_3$ on the surface of zeolite; The other is the existing acid active center on the surface of the zeolite molecular sieve. Although the reaction mechanism of this reaction is complicated with the previous zeolite molecular sieve catalysis, there are still many similarities in the overall reaction process. As shown in Figure 13, the anhydride first chemically adsorbed on the acid active center of the molecular sieve to form acyl carbocation, then attacked 2-MN to form active complex intermediates, and finally desorbed from the surface of the molecular sieve to form products. In addition, it can be seen from the characterization results that the acid content of the $AlCl_3$/Hβ catalyst increases with the increase of Cl content, indicating that the effective acid amount of the acid center formed by the bond between the molecular sieve surface and Cl is more, among which the medium and strong acids are very beneficial to the reaction.

4 Conclusion

In this article, the $AlCl_3$/Hβ catalysts are prepared by solvent reflux method using Hβ zeolite (Si/Al ratio of 25) as support. XRD results show that the prepared $AlCl_3$/Hβ catalyst has typical characteristic peaks and complete structure. SEM characterization shows that the molecular sieve loaded with $AlCl_3$ presents a small cube structure. With the increase in $AlCl_3$ concentration, more small particles are attached to the surface. BET results showed that the specific surface area of Hβ zeolite is increased, and pore volume and pore size are decreased by $AlCl_3$ fixation. XRF results show that immobilized $AlCl_3$ increases Al_2O_3 and Cl. NH_3-TPD and Py-IR showed that the $AlCl_3$/Hβ catalyst is mainly L-acid, and the acid content of B-acid also increases. With the increase in $AlCl_3$ concentration, the acid content of strong acid, medium strong acid, and weak acid all increase.

In the acylation of 2-MN with PA over $AlCl_3$/Hβ, the reaction activity and selectivity decrease with pore size and specific surface area and increase with Cl content and acid content. The results showed that when the concentration of $AlCl_3$ was 3 $g \cdot L^{-1}$, the concentration of reflux solvent was 8 h, and calcination at 550°C for 3 h, the catalytic activity of $AlCl_3$/Hβ was better. Under atmospheric pressure, $AlCl_3$/Hβ catalyst has higher catalytic activity in propionyl of 2-MN with TS as the solvent and 190°C for 10 h. Under this condition, the reaction has higher activity and selectivity. The conversion of 2-MN is 85.86%, and the yield of β,β-MPN is 81.19%.

In general, $AlCl_3$/Hβ catalyst can catalyze the acylation of 2-methylnaphthalene effectively. Compared with the traditional $AlCl_3$ catalyst, the amount of $AlCl_3$ used is greatly reduced, and the production cost is reduced. Moreover, the immobilization catalyst can be directly filtered and separated from the solution, simplifying the post-treatment steps, and reducing the generation of a large amount of waste acid and waste gas. It is a relatively environmentally friendly green catalyst.

Funding information: This work was financially supported by the National Natural Science Foundation of China (91634101) and The Project of Construction of Innovative Teams and Teacher Career Development for Universities and Colleges under Beijing Municipality (IDHT20180508).

Author contributions: Jingjing Sun: writing – original draft, writing – review and editing, methodology, formal analysis; Haibo Jin: writing – review and editing, resources, funding acquisition, conceptualization; Xuefeng Mao: formal analysis; Guangxiang He: writing – review and editing, methodology; Junfang Li: resources, validation; Zihao Yan: validation; Fating Hu: investigation; Lei Ma: formal analysis, investigation; Xiaoyan Guo: supervision; Suohe Yang: software.

Conflict of interest: Authors state no conflict of interest.

References

[1] Zhu H, Meyer MP. Cationic intermediates in Friedel-Crafts acylation: Structural information from theory and experiment. Chem Commun. 2010;47:409–1111. doi: 10.1039/c0cc02286a.
[2] Kreitman KM, Brewer SE, Rodden JB, Blackbourn RL, Brownscombe TF, Buechele JL et al. An integrated process for the production of 2,6-naphthalene dicarboxylic acid. US: 6448436; 2002.
[3] Xu HS, Song CY, Zhao JH, Wang LC, Gan W. Study on methylation of 2-methylnaphthalene with methanol over MFI type zeolite catalyst. Acta Petrolei Sin. 1999;15(1):52–6.
[4] Zhang CR, Zhou B. Progress in synthesis of 2,6-naphthalene dicarboxylic acid. Chem Adhes. 2012;34(06):54–517.

[5] Li JF, Mao XF, Hu FT, Li WB. Synthesis and characterization of 2-methyl-6-propoylnaphthalene. J China Coal Soc. 2020;45(12):4184–90.
[6] Ren XH, Yang HH, Zhe DM, Gao YJ. Application status and the prospect of polyethylene naphthalenediate. Petrkchem Techno. 2021;50(06):616–21.
[7] Pivsa-Art S, Okuro K, Miura M, Murata S, Nomura M. Acylation of 2-methoxynaphthalene with acyl chlorides in the presence of a catalytic amount of lewis acids. J Chem Soc Perkin Trans 1. 1994;13:1703–7. doi: 10.1039/P19940001703.
[8] Wang P, Jian XG. Synthesis of 2-methyl-6-acylnaphthalene. J Dalian Univ Technol. 2008;1:99–102. doi: 10.16411/j.cnki.issn1006-7736.2008.01.007.
[9] Yuan B, Li ZS, Liu YJ, Zhang SS. Liquid phase acylation of 2-methylnaphthalene catalyzed by H-beta zeolite. J Mol Catal A-Chem. 2007;280(1):210–8.
[10] Li WP, Yang SH, Guo XY, He GX, Jin HB. The effect of operating conditions on acylation of 2-methylnaphthalene in a microchannel reactor. Chin J Chem Eng. 2018;26(6):1307–11.
[11] Mu MM, Chen LG. Research progress in Friedel-Crafts acylation of aromatic hydrocarbons catalyzed by solid acids. Fine Chem. 2017;34(4):361–7 + 406. doi: 10.13550/j.jxhg.2017.04.001.
[12] Wu YH, Tian FQ, He M, He M, Cai TX. Isomerization of α-pinene over immobilized $AlCl_3$ catalysts. Chin J Catal. 2011;32(6–8):1138–42.
[13] Petre AL, Hoelderich WF, Gorbaty ML. Dodecylbenzene transformations: Dealkylation and disproportionation over immobilized ionic liquid catalysts. Appl Catal A Gen. 2009;363(1):100–8.
[14] Zhang FF, Wu GW, Li H, Zhou YB. Research progress of Friedel-Crafts acylation catalysts. Appl Chem Ind. 2020;49(7):1823–8 + 1834.
[15] Qiao XL, Hu XY, Fang Y. Research progress of Friedel-Crafts acylation catalysts. Chem Ind Eng Prog. 2012;31(12):2702–7.
[16] Bykov VI, Belyaev BA. A new preparation method for the alkylation catalysts of aromatic compounds based on immobilized $AlCl_3$. Kinet Catal. 2021;62(2):328–30.
[17] Cai TC, He M, Shi XZ, Wang XP, Han DX, Lv LH. A study on structural suitability of immobilized aluminum chloride catalyst for isobutene polymerization. Catal Today. 2001;69:291–6.
[18] Cai TC, He M. New approaches to immobilization of aluminum chloride on γ-Alumina and its regeneration after deactivation. Catal Lett. 2003;86:17–23.
[19] Hu XC, Foo ML, Chuah GK, Jaenicke S. Pore size engineering on MCM-41: Selectivity tuning of heterogenized $AlCl_3$: For the synthesis of linear alkyl benzenes. J Catal. 2000;195(2):412–5.
[20] Tang H, Liu ZJ, Ji M, Jia CY, He M, Cai TC. Alkylation of naphthalene with propylene over a fixed $AlCl_3$ catalyst. Ind Catal. 2010;18(11):62–5.
[21] Lu PF, Jiang L, Mi PK, Mi PK, Huang FL, Chen Q, et al. Study on the structure of $AlCl_3$ catalyst supported by Al_2O_3. Petrkchem Techno. 2010;39(6):616–9.
[22] Wang NN, Jiang S, Ji M, He M, Lin J, Cai TC. Preparation of $AlCl_3$ supported catalyst and its catalytic performance for 1-decene polymerization. Petrkchem Techno. 2006;5:479–82.
[23] Dube D, Royer S, On DT, Beland F, Kaliaguine S. Aluminum chloride grafted mesoporous molecular sieves as alkylation catalysts. Micropor Mesopor Mate. 2005;79:137–44.
[24] Han X, Guo YJ, Wu W. Progress in preparing and applying of supported Lewis acid catalysts. Petrkchem Techno. 2006;35(1):88–93.
[25] Wu YH, Tian FQ, He M, Cai TX. Isomerization of a-pinene over immobilized $AlCl_3$ catalysts. Chin J Catal. 2011;32(7):1138–42.
[26] Qi LL, Ji M, Wang XK, Min H, Cai T. $AlCl_3$/MCM-41 as a catalyst for isomerization of *Endo*-tricyclodecane. Chin J Catal. 2010;31(4):383–5.
[27] Wen J, You K, Zhao F, Jian J, Liu P, Ai Q, et al. $AlCl_3$ immobilized on silicic acid as efficient Lewis acid catalyst for highly selective preparation of dicyclohexylamine from the vapor phase hydroamination of cyclohexene with cyclohexylamine. Catal Commun. 2020;145:106–12.
[28] Jadhav AH, Chinnappan A, Hiremath V, Seo JG. Synthesis and characterization of $AlCl_3$ impregnated molybdenum oxide as heterogeneous nano-catalyst for the Friedel-Crafts acylation reaction in ambient condition. JNN. 2015;15(10):8243–50.
[29] Jiang T, Cheng J, Liu W. Sulfuric acid functional zirconium(or aluminum) incorporated mesoporous MCM-48 solid acid catalysts for alkylation of phenol with tertbutylalcohol. J Solid State Chem. 2014;218(2):71–80.
[30] Bai G, Han J, Zhang H, Liu C, Lan X, Tian F, et al. Friedel-Crafts acylation of anisole with octanoic acid over acid-modified zeolites. RSC Adv. 2014;4(52):27116–21.